Progress and Validation of Geant4 Based Radioactive Decay Simulation Using the Examples of Simbol-X and IXO

S. Hauf, M. Kuster, M.G. Pia, Z. Bell, U. Briel, R. Chipaux, D.H.H. Hoffmann, E. Kendziorra, P. Laurent, L. Strüder, C. Tenzer, G. Weidenspointner, A. Zoglauer

***Abstract*—The anticipated high sensitivity and the science goals of the next generation X-ray space missions, like the International X-ray Observatory or Simbol-X, rely on a low instrumental background, which in turn requires optimized shielding concepts. We present Geant4 based simulation results on the IXO Wide Field Imager cosmic ray proton induced background in comparison with previous results obtained for the Simbol-X LED and HED focal plane detectors. Our results show that an improvement in mean differential background flux compared to actually operating X-ray observatories may be feasible with detectors based on DEPFET technology. In addition we present preliminary results concerning the validation of Geant4 based radioactive decay simulation in space applications as a part of the Nano5 project.**

TABLE I
SIMBOL-X AND IXO MISSION PARAMETERS.

	Simbol-X	IXO
Concept	Formation flight	Expandable Bench
Focal Length	25 m	20 m
Energy Ranges	0.5–20 keV	0.1–15 keV
	5–80 keV	5–40 keV
Spatial Resolution	128×128 pixels	1024×1024 pixels
Angular Resolution	30”	5”
Pixel Size	625 μm	100 μm
Readout rate	4000 Hz	400 Hz

I. INTRODUCTION

THE next generation X-ray space missions like the International X-ray Observatory IXO, Simbol-X, NuStar or Astro-H aim to explore the X-ray sky in the energy range between 0.1 and 80 keV with so far unrivalled high sensitivity [1], [2]. To achieve this goal both missions require a low instrumental background which can only be realized with optimized shielding and background reduction techniques. To optimize the trade off between cost, weight, and performance of the detectors and shielding components, extensive and reliable Monte-Carlo simulations are necessary. Most of the state-of-the-art approaches to estimate the prompt cosmic rays, solar proton and the cosmic X-ray induced background in space rely on simulations with the Geant4 Monte Carlo toolkit [3], [4]. The Geant4 electromagnetic and hadronic physics models have extensively been verified not only with space but also with ground based experiments. In contrast measurements to verify the radioactive decay implementation in Geant4 have been rare or have only been tested on a limited set of isotopes, which are not necessarily those used in satellite construction. On the other hand, measured background data of actual and past missions (e.g. INTEGRAL) show that up to 20% of the instrumental background can be due to long term activation of the detector materials in orbit [5], [6]. This necessitates that the delayed background component is also taken into account, well understood and verified with laboratory measurements. While the background estimates for Simbol-X and IXO presented in this work are focused on the prompt cosmic ray proton induced background and optimizing the detector shielding against resulting secondary particles, we also present a first comparision of the radioactive decay physics implementation in Geant4 with experimental measurements.

Manuscript received November 20, 2009.

S. Hauf, M. Kuster and D.H.H. Hoffmann are with TU Darmstadt, Institut für Kernphysik, Schlossgartenstrasse 9, D-64289 Darmstadt, Germany

M.G. Pia is with European Organization for Nuclear Research (CERN), CH-1211 Genève 23, Switzerland and INFN, Sezione di Genova, Genova, Italy

Z. Bell is with Oak Ridge National Laboratry, Oak Ridge, TN, USA

U. Briel is with Max-Planck-Institut für extraterrestrische Physik, Giessenbachstrasse, D-85748 Garching, Germany

R. Chipaux and P. Laurent are with CEA/DSM/IRFU, Centre de Saclay, F-91191 Gif sur Yvette, France

E. Kendziorra and C. Tenzer are with Institut für Astronomie und Astrophysik Tübingen, Sand 1, D-72076 Tübingen

L. Strüder is with MPI Halbleiterlabor, Otto-Hahn-Ring 6, D-81739, Munich, Germany and Max-Planck-Institut für extraterrestrische Physik, Giessenbachstrasse, D-85748 Garching, Germany

G. Weidenspointner is with MPI Halbleiterlabor, Otto-Hahn-Ring 6, D-81739, Munich, Germany

A. Zoglauer is with University of California, Space Science Laboratory, Berkeley, USA

II. THE SIMBOL-X LOW AND HIGH ENERGY DETECTOR

The Simbol-X spacecraft is a planned X-ray observatory sensitive in the energy range between 0.1 to 80 keV [7], [8]. Focusing X-rays up to this energy range requires a focal length of around 20 m. Because a satellite this large would be problematic to launch with available launch systems, Simbol-X will consist of two spacecrafts in close formation flight. The Simbol-X focal plane consists of two detectors which cover the full energy range with a maximum possible sensitivity.

The Simbol-X Low Energy Detector (LED) is a 450 μm thick, fully depleted DEPFET macro-pixel detector sensitive in the energy range of 0.5–20 keV [9]. The current detector design provides an energy resolution of $E/\Delta E = 40$–50 at 6–10 keV [10]. The major advantages of this monolithic devices

are there homogeneous entrance window, a filling factor of 100%, the fast read-out and a quantum efficiency above 98% between 1 and $10\,\mathrm{keV}$. Furthermore, the DEPFET concept allows to reduce the power consumption of the detector to a necessary minimum, since the amplifiers of the individual pixels need only be powered during read-out. The detector area is also homogeneously transparent which allows for placing detectors sensitive in higher energy ranges underneath. In the case of Simbol-X this is a CdTe High Energy Detector (HED) sensitive in the 5–80 keV range [10]. The Simbol-X LED detector is subdivided into 128×128 pixels with a size of $625 \times 625\,\mu\mathrm{m}^2$ providing an angular resolution of 30 arc seconds oversampling the mirror resolution by a factor of 3. The smallness of the LED detector allows a high read-out rate of $8000\,\mathrm{Hz}$ making it possible to combine the detector with an active anti-coincidence system, reducing the particle induced background by an order of magnitude [11]. To suppress secondary X-rays in the detector energy range of interest, induced by particle and gamma-ray interactions in the detector materials, the focal plane detector assembly is surrounded by a graded-Z shield consisting of layers of tantalum, tin, copper, aluminum and a carbon-composite material. For simulations the LED and HED along with their surrounding shielding, the anti-coincidence and support structures were modelled. The satellite structure and auxiliary systems were replaced by a bulk aluminum mass with an expected mean density. Data post-processing included proper anti-coincidence treatment, as well as pattern and MIP analysis similar to the pattern recognition and MIP rejection algorithm actually implemented in the EPIC pn-camera event analyzer on board of XMM-Newton [12].

III. The Wide Field Imager and Hard X-ray Imager of IXO

The International X-ray Observatory (IXO) is a joint project of the space agencies ESA, NASA and JAXA with the goal to develop a next generation low background X-ray telescope with high resolution imaging and spectroscopic observations up to $40\,\mathrm{keV}$. The combination of these performance parameters requires a large effective telescope area in combination with a low instrumental background. The core IXO imaging instrument for the 0.1–$15\,\mathrm{keV}$ energy range will be the Wide Field Imager (WFI). The WFI concept follows a similar design as the Simbol-X LED, i.e. silicon drift detector macro-pixels with a DEPFET read-out. The detector consists of a 1024×1024 pixel array with $100 \times 100\mu\mathrm{m}^2$ pixel size. The better mirror resolution in combination with the smaller pixel size of the WFI as compared to Simbol-X leads to an angular resolution of 3 arc seconds in the energy range of 0.1–$15\mathrm{keV}$ [13]. The larger amount of pixels will result in a higher data rate, which reduces the feasible read-out rate due to power, telemetry and on board data handling capacity from 8000 to $400\mathrm{Hz}$. At this read-out speed an active anti-coincidence is rather unrealistic since it would result in a dead time beyond 50%. Similar to the Simbol-X LED design it is planned to implement a graded-Z shield which is currently being optimized in the course of our simulations.

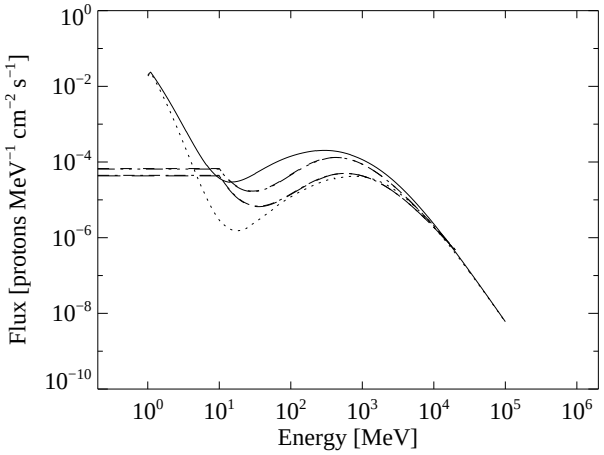

Fig. 1. Spectral distribution of cosmic ray protons based on the CREME96 and CREME86 space radiation models for different mission and orbital parameters. From top to bottom (at 100 MeV) proton spectra assuming the following models and launch dates are shown: CREME96 for the IXO orbit assuming 2020 as launch date, CREME86 for IXO orbit assuming 2020 as launch date, CREME86 for the IXO orbit assuming 2013 as launch date and CREME96 for the IXO orbit assuming 2013 as launch date. The two CREME86 Simbol-X orbit models are not distinguishable from their IXO counterparts.

The IXO Hard X-ray Imager (HXI) will cover photon energies up to $40\,\mathrm{keV}$ with a 1024×1024 pixel CdTe detector array. It takes advantage of the fact that the WFI is homogeneously transparent in this energy range. It will have the same pixel geometry and spatial resolution as the WFI allowing for simultaneous spectra imaging using both detectors. A comparison between the satellite concepts of IXO and Simbol-X can be found in Table I.

IV. The Cosmic Ray Spectrum at L2

The IXO spacecraft will be positioned at the L 2 Lagrange point, at a distance of approximately $1.5 \times 10^6\,\mathrm{km}$ from the Earth. Due to the lack of Earth's geomagnetic shielding the satellite and the detectors will be subject to cosmic ray impacts, modulated in intensity by the solar cycle. The IXO orbit allows to point the spacecraft in such a way, that the FOV is always facing away from the Sun, thus theoretically allowing continuous observations. To characterize the radiation background at L 2 we rely on model estimates for the cosmic ray flux for our simulation. We use the CREME96 model [14] with a fixed distance of $1.5 \times 10^6\,\mathrm{km}$ above Earth for the planned launch date in 2020. This date is near the solar cycle minimum, corresponding to a cosmic ray flux maximum. Furthermore, we concentrate on the proton contribution of the total cosmic ray flux, which is by far the most dominant component. According to [14] the CREME model is valid out to Mars orbit, which is at a distance from the Sun well beyond L 2.

Fig. 1 shows a comparison between the cosmic ray proton spectrum calculated from different CREME models for both missions Simbol-X and IXO and different launch dates. It is apparent that in contrast to the older CREME86 model [15], the CREME96 model gives a larger flux variation due to the

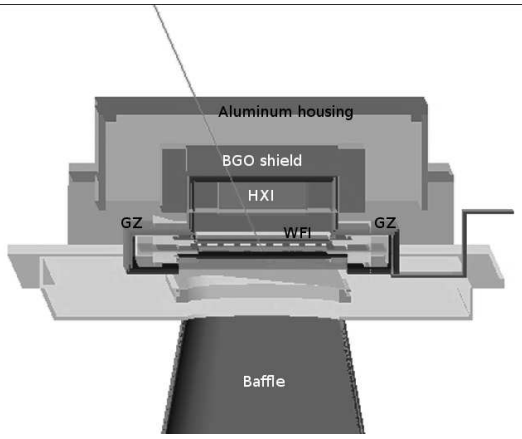

Fig. 2. The Geant4 baseline geometry of the WFI and HXI detectors. The following components are shown from the outer to the inner: the aluminum housing, the BGO shield, the graded-Z shield, the HXI and the macro-pixel detector of the WFI.

influence of the solar cycle. Please note, that the Simbol-X launch date of 2013 is near the solar maximum (cosmic ray minimum) and the planned IXO launch date of 2020 is close the solar minimum (cosmic ray maximum). The satellite orbital position seems to have a negligible effect on the resulting proton spectrum.

V. Geant4 Simulations

The actual background simulations for IXO were done with the Geant4 Monte-Carlo software environment developed at CERN. Similar to Simbol-X, we transfered the IXO detector geometry from the baseline mechanical engineering model, abstracting some components in the process in order to reduce computing time to a necessary minimum. The Si wafer of the WFI and surrounding read-out electronics were modelled with greatest detail, while the level of detail was reduced for more distant geometry components. A graded-Z shield consisting of layers of tantalum, tin, copper, aluminum and carbon was included in the model as the innermost layers close to the wafer. The satellite structure was modelled assuming a simplified geometry representation of the movable and fixed instrument platform as well as the Sun shield. This baseline geometry, without the satellite structures, is shown in Fig. 2 and will be used as a basis for further design iterations and optimizations aimed at reducing the detector particle background.

Our simulations for Simbol-X and IXO are based on the same standard electromagnetic and low energy electromagnetic [16] Geant4 models, as well as a full set of hadronic physics which have already been used for our Simbol-X simulations [12]. The simulation of activation and radioactive decay processes is optional. Our current simulations were done using Geant 4.9.2 p01.

Additional background reduction can be realized during data post-processing by analysing pixel patterns and energy deposition of events in the detector. An event is only considered as valid if it meets certain criteria: the pixel pattern and the energy distribution attributed to the event must fit into a specified valid pattern mask. Furthermore, the deposited energy must be

TABLE II
Background estimates for Simbol-X and IXO.

	Simbol-X	IXO
Readout rate	4000 Hz	400 Hz
Anti-coincidence	yes	no
Raw count rate[1]	175	2800
Count rate after AC[1]	5.25 ± 0.88	NA
Count rate after pattern analysis[1]	2.00 ± 0.55	77 ± 3.7
AC induced dead time	18.7%	NA
Efficiency AC	97%	NA
Efficiency pattern analysis.	62%	97%

[1] count rates are given in units of $10^{-4}\mathrm{cts\,cm^{-2}\,s^{-1}\,keV^{-1}}$

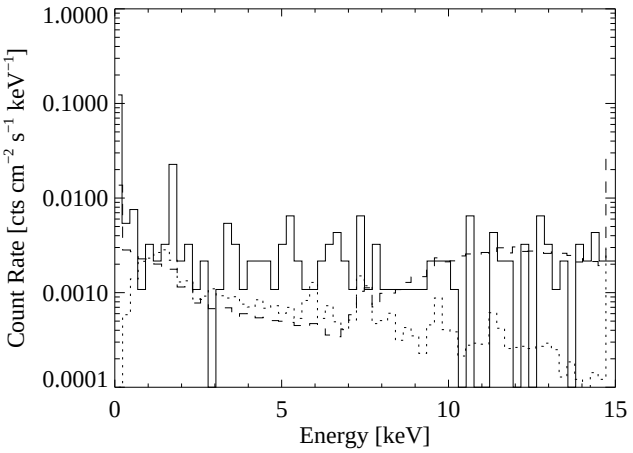

Fig. 3. Simulated IXO WFI differential background spectrum (solid line) in comparison to the measured blank sky background of the Suzaku back (dashed line) and front illuminated CCDs of the XIS detector (dotted line) [17].

below a minimum ionizing particle (MIP) threshold currently set to 15 keV, which is the maximum of the WFI energy range. For the case that an invalid event pattern was registered in one read-out frame, we have investigated the efficiency of different algorithms to reject the event pattern: discarding only the affected pixels or the complete frame in which the event was included. The discarding of whole frames approximately halves the background rate but also introduces a dead time of around 50%. Due to this only single patterns will be discarded in future simulations. For test purposes we have also included a simplified geometric representation of the XMS experiment, a microcalorimeter spectrometer, in our model, in order to study it's influence on the WFI background.

VI. Simulation Results: Prompt proton induced background

Our simulations for Simbol-X yield a count rate of $(2.0 \pm 0.6) \times 10^{-4}\mathrm{cts\,cm^{-2}\,s^{-1}\,keV^{-1}}$ for the LED with 18.7% down time and $(2.6 \pm 0.3) \times 10^{-4}\mathrm{cts\,cm^{-2}\,s^{-1}\,keV^{-1}}$ for the HED [11]. The countrates given are with proper anti-coincidence treatment and pattern analysis applied and are well within the envisioned rates.

For IXO our simulations yield a preliminary estimate of the WFI background in the $10^{-3}\,\mathrm{cts\,cm^{-2}\,s^{-1}\,keV^{-1}}$ range for

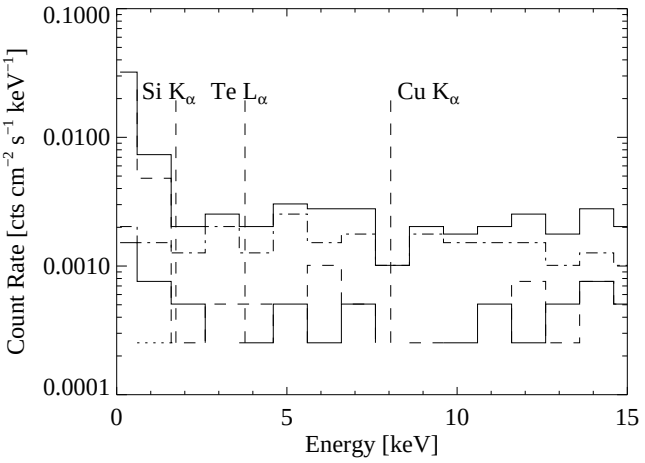

Fig. 4. Simulated differential background spectrum of the WFI detector after pattern and MIP analysis. From top to bottom the following spectra are shown: the total background spectrum (solid line) and the contribution of electrons (dash-dotted line), gammas (solid line) and protons (dashed line) to the total background spectrum. For a detailed description see text.

Fig. 5. Experimental setup to measure the decay spectra of different isotopes (see text). On the left hand side the germanium spectrometer covered by a lead shielding is shown. The radioactive isotopes where placed into the gap between the spectrometer and the metal boxes on the left.

the baseline geometry. This background level is one order of magnitude above the envisioned rate of $10^{-4}\,\mathrm{cts\,s^{-1}\,keV^{-1}}$ and consistent with background rates observed by currently flying missions like Suzaku as shown in Fig. 3. At the present level of detail and statistics, the influence of the XMS on the WFI background is negligible.

Our results show that the pattern and MIP detection algorithms used can reliably reject 96% of the background as invalid patterns. The remaining 4% of the overall background mainly originates from secondary electron and primary proton energy depositions in the WFI silicon chip as shown in the background spectrum in Fig. 4. Of these valid event patterns 74% are single pixel events, 24% are double pixel events and a remaining fraction of 2% are triple pixel events. While events with $n > 3$ dominate the raw background rate, they either have invalid pattern shapes or deposit an energy which is above the MIP threshold or commonly both. Furthermore, we observe a reduction of the background of approximately 50% in the case that we discard a complete frame if a invalid event pattern is observed in this frame. Though this roughly halves the background rate it also introduces a dead time of $> 50\%$.

The WFI background spectrum shown in Fig. 4 also demonstrates that the actual design of the graded-Z shield effectively reduces any emission lines. Since electrons are the most prominent source of the remaining background, which are not detectable through the applied pattern or MIP rejection algorithms, future optimisation of the mechanical design will focus on this issue.

VII. Progress of the Validation of Geant4 Radioactive Decay Simulations

Our previous simulations for the Simbol-X focal plane detector module yield an increase of the HED mean differential background flux due to activation by cosmic ray protons from $2.6 \times 10^{-4}\,\mathrm{cts\,cm^{-2}\,s^{-1}\,keV^{-1}}$ to $3.34 \times 10^{-4}\,\mathrm{cts\,cm^{-2}\,s^{-1}\,keV^{-1}}$ [11], [12], [18], [19]. Since we expect a larger incident cosmic ray proton flux for the IXO mission time window and orbit in comparison to the Simbol-X mission, we consequently assume that the proton induced prompt and delayed background due to activation will contribute with a similar or even larger amount to the total detector background of the WFI. This assumption requires that we have an accurate treatment of this background component in our simulations. Experience with existing Geant extensions like MGGPOD (Geant3) and Cosima (Geant4) [20], [21] further supports this assumption.

Because data on a systematic experimental verification of the radioactive decay physics implemented in Geant4 has been rare, we have started an experimental validation of the radioactive decay physics as part of the Nano5 project [22]. In a first simple and straight forward approach, we tried to reproduce measured spectra of different radioactive sources with Geant4. The isotopes we used were ^{137}Cs, ^{22}Na, ^{54}Mn, ^{60}Co, ^{57}Co and ^{133}Ba, with a specified activity of $37\,\mathrm{kBq}$ in June 2006. The decay spectrum of each individual isotope was observed with an ORTEC GEM70P4 high purity Germanium detector with a $500\mu\mathrm{m}$ thick Beryllium entrance window [23]. The detector provides an energy resolution of $1\,\mathrm{keV}$ at $122\,\mathrm{keV}$ and $2\,\mathrm{keV}$ at $1.33\,\mathrm{MeV}$ and was covered by a pair of copper and tin tubes and additional lead shielding in order to suppress environmental gamma ray induced background. The sources were placed at a known distance in a gap between the detector and shielding components as shown in Fig. 5. A background measurement was conducted before and after each source measurement. The experimental spectra were subsequently background subtracted and binned into $1\,\mathrm{keV}$ energy intervals.

The geometry of the experimental setup, including all shielding elements, and detector components was implemented as a Geant4 geometry following the information provided by ORTEC [priv. comm.]. For our simulations we induced 10^6

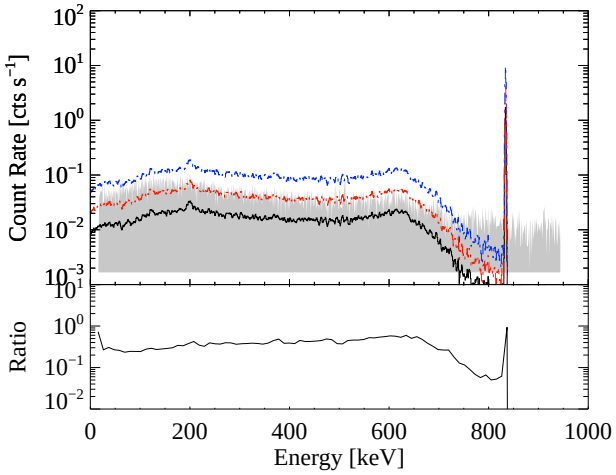

Fig. 6. Experimentally measured and background subtracted ^{54}Mn spectrum (grey shaded region) in comparison to simulated spectra. The simulated spectrum has been normalized to the activity of the source (bottom line, black), the continuum (middle line, orange) and the peaks (top line, blue). Notice the difference in the peak to continuum ratio.

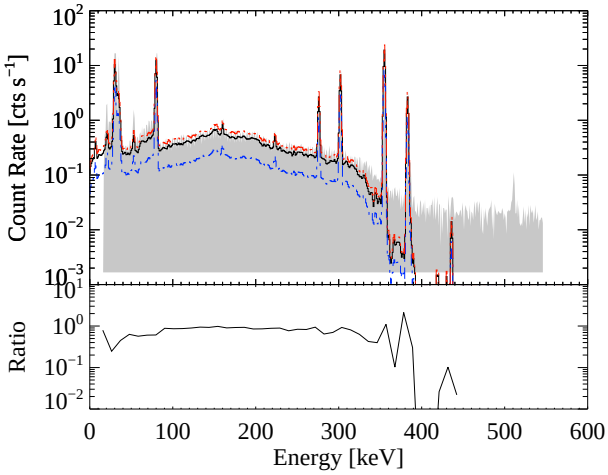

Fig. 7. Experimentally measured and background subtracted ^{133}Ba spectrum (grey shaded region) in comparison to simulated spectra. The simulated spectrum has been normalized to the activity of the source (middle line, black), the continuum (top line, orange) and the peaks (bottom line, blue). Notice the difference in peak to peak ratios.

decays for each isotope using the same electromagnetic and hadronic physics as for our Simbol-X and IXO background simulations. The source was modelled to emit to a solid angle of 4π. The simulated spectra were binned in the same way as the measured spectra and finally normalized to the isotope's calculated activity on the measurement date, using an activity of $37\,\mathrm{kBq}$ in June 2006 as a reference point. The detector energy resolution was approximated by folding the simulated data with a Gaussian function.

Two examples of our results, a comparison of measured and simulated spectra of two isotopes, ^{54}Mn and ^{133}Ba, are shown in Figs. 6, 7. It is obvious from Figs. 6, 7 that the simulation is able to qualitatively reproduce most of the spectral features (continuum shape and emission lines). On the other hand there is a clear disagreement between peak to peak and peak to continuum ratios by a factor of up to 3 between the simulated and measured spectra. In case of ^{54}Mn the mean ratio of simulated data to experimental data is 0.3 for the continuum compared to 0.9 for the peak. Our comparision for ^{133}Ba shows peak ratios varying between 0.6 and 1.0. This disagreement has been observed for all measured isotopes, at different levels.

While there remains a systematic uncertainty in our flux normalisation of the simulated data due to small uncertainties of the detector to source distance or of the activity of the sources which affect the overall normalization of the measured spectra, such a disagreement of the peak to peak and peak to continuum ratios could be of more serious nature and should be further investigated. Currently we are focusing on two possibilities: either our Geant4 model is over-simplified and we are missing important geometry parts or there is an underlying problem in Geant4 physics.

Further measurements are currently in progress to investigate if this problem exists for a broader variety of isotopes. At the same time we investigate the influence of different geometrical parameters in the simulation in order to quantify their influence on the result. Along with analysing the contributions of the individual physics processes involved this will lead to a better understanding of the origin of the observed discrepancies.

VIII. Conclusions and Outlook

Our background estimates for the Simbol-X LED detector have demonstrated that background rates in the $10^{-4}\,\mathrm{cts\,cm^{-2}\,s^{-1}\,keV^{-1}}$ range are achievable with the DEPFET detector technology. Preliminary simulation results for the IXO WFI detector yield a background level which is significantly larger compared to the anticipated science goal and consequently the present baseline WFI design requires further optimisation.

In parallel to this work we are currently undertaking an experiment with laser accelerated protons with the goal to measure the proton induced activation and decay spectra of different graded-Z shield materials which will be used for the IXO WFI.

Acknowledgement

This work is supported by the Bundesministerium für Wirtschaft und Technologie and the Deutsches Zentrum für Luft- und Raumfahrt - DLR under the grant number 50QR0902.

References

[1] J. E. Koglin, H. An, K. L. Blaedel, N. F. Brejnholt, F. E. Christensen, W. W. Craig, T. A. Decker, C. J. Hailey, L. C. Hale, F. A. Harrison, C. P. Jensen, K. K. Madsen, K. Mori, M. J. Pivovaroff, G. Tajiri, and W. W. Zhang, "NuSTAR hard x-ray optics design and performance," in *Society of Photo-Optical Instrumentation Engineers (SPIE) Conference Series*, ser. Presented at the Society of Photo-Optical Instrumentation Engineers (SPIE) Conference, vol. 7437, Aug. 2009.

[2] T. Takahashi, R. Kelley, K. Mitsuda, H. Kunieda, R. Petre, N. White, T. Dotani, R. Fujimoto, Y. Fukazawa, K. Hayashida, M. Ishida, Y. Ishisaki, M. Kokubun, K. Makishima, K. Koyama, G. M. Madejski, K. Mori, R. Mushotzky, K. Nakazawa, Y. Ogasaka, T. Ohashi, M. Ozaki, H. Tajima, M. Tashiro, Y. Terada, H. Tsunemi, T. G. Tsuru, Y. Ueda, N. Yamasaki, S. Watanabe, and the NeXT team, "The next mission," 2008. [Online]. Available: http://www.citebase.org/abstract?id=oai:arXiv.org:0807.2007

[3] S. Agostinelli, J. Allison, K. Amako, J. Apostolakis, H. Araujo, P. Arce, M. Asai, D. Axen, S. Banerjee, G. Barrand, F. Behner, L. Bellagamba, J. Boudreau, L. Broglia, A. Brunengo, H. Burkhardt, S. Chauvie, J. Chuma, R. Chytracek, G. Cooperman, G. Cosmo, P. Degtyarenko, A. dell'Acqua, G. Depaola, D. Dietrich, R. Enami, A. Feliciello, C. Ferguson, H. Fesefeldt, G. Folger, F. Foppiano, A. Forti, S. Garelli, S. Giani, R. Giannitrapani, D. Gibin, J. J. Gómez Cadenas, I. González, G. Gracia Abril, G. Greeniaus, W. Greiner, V. Grichine, A. Grossheim, S. Guatelli, P. Gumplinger, R. Hamatsu, K. Hashimoto, H. Hasui, A. Heikkinen, A. Howard, V. Ivanchenko, A. Johnson, F. W. Jones, J. Kallenbach, N. Kanaya, M. Kawabata, Y. Kawabata, M. Kawaguti, S. Kelner, P. Kent, A. Kimura, T. Kodama, R. Kokoulin, M. Kossov, H. Kurashige, E. Lamanna, T. Lampén, V. Lara, V. Lefebure, F. Lei, M. Liendl, W. Lockman, F. Longo, S. Magni, M. Maire, E. Medernach, K. Minamimoto, P. Mora de Freitas, Y. Morita, K. Murakami, M. Nagamatu, R. Nartallo, P. Nieminen, T. Nishimura, K. Ohtsubo, M. Okamura, S. O'Neale, Y. Oohata, K. Paech, J. Perl, A. Pfeiffer, M. G. Pia, F. Ranjard, A. Rybin, S. Sadilov, E. di Salvo, G. Santin, T. Sasaki, N. Savvas, Y. Sawada, S. Scherer, S. Sei, V. Sirotenko, D. Smith, N. Starkov, H. Stoecker, J. Sulkimo, M. Takahata, S. Tanaka, E. Tcherniaev, E. Safai Tehrani, M. Tropeano, P. Truscott, H. Uno, L. Urban, P. Urban, M. Verderi, A. Walkden, W. Wander, H. Weber, J. P. Wellisch, T. Wenaus, D. C. Williams, D. Wright, T. Yamada, H. Yoshida, and D. Zschiesche, "Geant4- a simulation toolkit," *Nucl. Instrum. Methods Phys. Res., Sect. A*, vol. 506, pp. 250–303, Jul. 2003. [Online]. Available: http://www.cern.ch/geant4

[4] J. Allison, K. Amako, J. Apostolakis, H. Araujo, P. Arce Dubois, M. Asai, G. Barrand, R. Capra, S. Chauvie, R. Chytracek, G. A. P. Cirrone, G. Cooperman, G. Cosmo, G. Cuttone, G. G. Daquino, M. Donszelmann, M. Dressel, G. Folger, F. Foppiano, J. Generowicz, V. Grichine, S. Guatelli, P. Gumplinger, A. Heikkinen, I. Hrivnacova, A. Howard, S. Incerti, V. Ivanchenko, T. Johnson, F. Jones, T. Koi, R. Kokoulin, M. Kossov, H. Kurashige, V. Lara, S. Larsson, F. Lei, O. Link, F. Longo, M. Maire, A. Mantero, B. Mascialino, I. McLaren, P. Mendez Lorenzo, K. Minamimoto, K. Murakami, P. Nieminen, L. Pandola, S. Parlati, L. Peralta, J. Perl, A. Pfeiffer, M. G. Pia, A. Ribon, P. Rodrigues, G. Russo, S. Sadilov, G. Santin, T. Sasaki, D. Smith, N. Starkov, S. Tanaka, E. Tcherniaev, B. Tome, A. Trindade, P. Truscott, L. Urban, M. Verderi, A. Walkden, J. P. Wellisch, D. C. Williams, D. Wright, and H. Yoshida, "Geant4 developments and applications," *IEEE Transactions on Nuclear Science*, vol. 53, pp. 270–278, Feb. 2006.

[5] P. Jean, J. E. Naya, and P. von Ballmoos, "Performance of an integral spectrometer model," in *The Transparent Universe*, ser. ESA Special Publication, . P. D. C. Winkler, T. J.-L. Courvoisier, Ed., vol. 382, 1997, pp. 635–+.

[6] P. Jean, G. Vedrenne, J. P. Roques, V. Schönfelder, B. J. Teegarden, A. von Kienlin, J. Knödlseder, C. Wunderer, G. K. Skinner, G. Weidenspointner, D. Attié, S. Boggs, P. Caraveo, B. Cordier, R. Diehl, M. Gros, P. Leleux, G. G. Lichti, E. Kalemci, J. Kiener, V. Lonjou, P. Mandrou, P. Paul, S. Schanne, and P. von Ballmoos, "Spi instrumental background characteristics," *A&A*, vol. 411, pp. L107–L112, Nov. 2003.

[7] P. Ferrando, M. Arnaud, B. Cordier, A. Goldwurm, O. Limousin, J. Paul, J. L. Sauvageot, P.-O. Petrucci, M. Mouchet, G. F. Bignami, O. Citterio, S. Campana, G. Pareschi, G. Tagliaferri, U. G. Briel, G. Hasinger, L. Strüder, P. Lechner, E. Kendziorra, and M. J. L. Turner, "Simbol-x: a new-generation hard x-ray telescope," in *Optics for EUV, X-Ray, and Gamma-Ray Astronomy. Edited by Citterio, Oberto; O'Dell, Stephen L. Proceedings of the SPIE, Volume 5168, p p. 65-76 (2004).*, ser. Presented at the Society of Photo-Optical Instrumentation Engineers (SPIE) Conference, O. Citterio and S. L. O'Dell, Eds., vol. 5168, Feb. 2004, pp. 65–76.

[8] P. Ferrando, A. Goldwurm, P. Laurent, O. Limousin, J. Martignac, F. Pinsard, Y. Rio, J. P. Roques, O. Citterio, G. Pareschi, G. Tagliaferri, F. Fiore, G. Malaguti, U. Briel, G. Hasinger, and L. Strüder, "Simbol-x: a formation-flying mission for hard-x-ray astrophysics," in *Optics for EUV, X-Ray, and Gamma-Ray Astronomy II. Edited by Citterio, Oberto; O'Dell, Stephen L. Proceedings of the SPIE, Volume 5900, pp. 195-204 (2005).*, ser. Presented at the Society of Photo-Optical Instrumentation Engineers (SPIE) Conference, O. Citterio and S. L. O'Dell, Eds., vol. 5900, Aug. 2005, pp. 195–204.

[9] P. Lechner, R. Hartmann, P. Holl, G. Lutz, N. Meidinger, R. H. Richter, H. Soltau, and L. Strüder, "X-ray imaging spectrometers in present and future satellite missions," *Nucl. Instrum. Methods Phys. Res., Sect. A*, vol. 509, pp. 302–314, Aug. 2003.

[10] P. Ferrando, "Simbol-x, an x-ray telescope for the 0.5-70 kev range," in *SF2A-2002: Semaine de l'Astrophysique Francaise*, F. Combes and D. Barret, Eds., Jun. 2002, pp. 271–+.

[11] C. Tenzer, U. Briel, A. Bulgarelli, R. Chipaux, A. Claret, G. Cusumano, E. Dell'Orto, V. Fioretti, L. Foschini, S. Hauf, E. Kendziorra, M. Kuster, P. Laurent, and A. Tiengo, "Status of the simbol-x background simulation activities," in *American Institute of Physics Conference Series*, ser. American Institute of Physics Conference Series, J. Rodriguez & P. Ferrando, Ed., vol. 1126, May 2009, pp. 75–78.

[12] S. Hauf, "Simulation on the simbol-x detector background," Master's thesis, TU Darmstadt, Mar. 2009.

[13] A. Stefanescu, M. Bautz, D. Burrows, L. Bombelli, C. Fiorini, G. Fraser, K. Heinzinger, S. Hermann, M. Kuster, T. Lauf, P. Lechner, G. Lutz, P. Majewski, S. Murray, M. Porrp, R. Richer, A. Santangelo, G. Schaller, M. Schnecke, F. Schoper, H. Soltau, L. Strüder, J. Treis, H. Tsunemi, G. de Vita, and J. Wilms, "The wide-field imager of the international x-ray observatory," *Nucl. Instrum. Methods Phys. Res., Sect. A*, 2009, submitted.

[14] A. Tylka, W. Dietrich, P. Boberg, E. Smith, J. Adams, Jr., B. Brownstein, E. Flueckinger, E. Petersen, S. M.A., and D. Smart, "Creme96: A revision of the cosmic ray effects on micro-electronics code," *IEEE Trans. Nucl. Sci.*, pp. 2150–2160, 1997.

[15] J. H. J. Adams, "Cosmic ray effects on miecro-electronics (creme), part iv," Naval Research Laboratory Memorandum Report 5901, December 1986.

[16] J. Apostolakis, S. Giani, M. Maire, P. Nieminen, M. Pia, and L. Urban, "Geant4 low energy electromagnetic models for electrons and photons," 1999.

[17] NASA, "Xis blank sky background files," Downloadable FITS, November 2009.

[18] C. Tenzer, E. Kendziorra, A. Santangelo, M. Kuster, P. Ferrando, P. Laurent, A. Claret, and R. Chipaux, "Monte carlo simulations of stacked x-ray detectors as designed for simbol-x," in *Space Telescopes and Instrumentation II: Ultraviolet to Gamma Ray*, ser. Proceedings of SPIE, M. J. L. Turner and G. Hasinger, Eds., vol. 6266, Jul. 2006.

[19] R. Chipaux, U. Briel, A. Bulgarelli, L. Foschini, E. Kendziorra, C. Klose, M. Kuster, P. Laurent, and C. Tenzer, "Status of the simbol-x detector background simulation activities." *Memorie della Societa Astronomica Italiana*, vol. 79, pp. 234–+, 2008.

[20] G. Weidenspointner, M. J. Harris, C. Ferguson, S. Sturner, and B. J. Teegarden, "Mggpod: a monte carlo suite for modelling instrumental backgrounds in [gamma]-ray astronomy and its application to wind/tgrs and integral/spi," *New Astronomy Reviews*, vol. 48, no. 1-4, pp. 227 – 230, 2004, astronomy with Radioactivities IV and Filling the Sensitivity Gap in MeV Astronomy. [Online]. Available: http://www.sciencedirect.com/science/article/B6VNJ-4B72877-3/2/1e75fcbfbdf488e810

[21] A. Zoglauer *et al.*, "Megalib - medium energy gamma-ray astronomy library," 2005.

[22] M. Augelli, M. Begalli, T. Evans, E. Gargioni, S. Hauf, C. Kim, M. Kuster, M. Pia, P. Queiroz Filho, L. Quintieri, P. Saracco, D. Souza Santos, D. Weidenspointner, and A. Zoglauer, "Geant4-related r&d for new particle transport methods," Dec. 2009, this volume.

[23] *GEM Series Coaxial HPGe Detectors Configuration Guide*, ORTEC, 801 South Illinois Ave.,Oak Ridge,TN 37831-0895 U.S.A.